JVSTA
JOURNAL OF VACUUM SCIENCE AND TECHNOLOGY A

Population and alignment of N2 scattered from Ag(111)

Greg O. Sitz, Andrew C. Kummel, and Richard N. Zare

Citation: J. Vac. Sci. Technol. A **5**, 513 (1987); doi: 10.1116/1.574703
View online: http://dx.doi.org/10.1116/1.574703
View Table of Contents: http://avspublications.org/resource/1/JVTAD6/v5/i4
Published by the AVS: Science & Technology of Materials, Interfaces, and Processing

Population and alignment of N_2 scattered from Ag(111)

Greg O. Sitz, Andrew C. Kummel, and Richard N. Zare
Department of Chemistry, Stanford University, Stanford, California 94305

(Received 22 September 1986; accepted 27 October 1986)

A well-characterized Ag(111) surface in an ultrahigh vacuum system is bombarded with supersonically cooled N_2 and the scattered molecules are detected near the specular angle using $2+2$ resonance enhanced multiphoton ionization. The first three even spatial moments of the angular momentum distribution have been measured. The zeroth moment is the population of a given rotational level, while the second and fourth moments describe the quadrupole and hexadecapole alignment of the J vector with respect to the surface normal. The relative population distribution shows an excess at high J characteristic of rotational rainbow scattering. For $J>7$, the second and fourth moments closely approach their limiting values expected when the J vector lies in the plane of the surface. It is concluded that the N_2/Ag(111) system closely approaches the ideal of a rigid rotor colliding with a flat surface.

I. INTRODUCTION

Molecular beam studies of inelastic scattering of molecules from solid surfaces have proven to be useful in elucidating the nature of the gas–surface interaction potential.[1] In the large majority of experimental studies the emphasis has been on determining internal state distributions, primarily rotational distributions, rather than on the angular momentum spatial distribution. The population of a quantum state is a scalar quantity, that is, a number with no additional information. The angular momentum of that state is a vector quantity, and the orientation in space of the vector as well as its length provide information on the forces that gave rise to the state. The present study is motivated by the possibility that measurements of the spatial distribution of the angular momentum vectors of surface-scattered molecules will yield detailed information on the forces acting during the molecule–surface encounter.

In this article we report measurements of the first three even moments of the angular momentum distribution of N_2 scattered from Ag(111). The scattered N_2 is detected in a quantum state specific manner by $2+2$ resonance enhanced multiphoton ionization (REMPI). This technique has been used to determine rotational population distributions in N_2 at higher pressure (0.05–0.50 Torr)[2] and we have extended this method to lower pressure (1×10^{-8} Torr).

There has been only one previous study of the alignment of molecules scattered from a well-characterized single-crystal surface. Klein, *et al.*[3] have reported the polarization of NO scattered from Ag(111) determined by laser-induced fluorescence. They measured the second moment of the NO angular momentum distribution and found the scattered NO to be aligned with its J vector pointing preferentially in a plane parallel to the surface. At low values of J ($J<15$) they found small alignment, at higher J values the alignment increased to a maximum value of $A_0^{(2)}=-0.75$ for $20.5<J<35.5$, and at the highest J ($J>40.5$) it was again small. Subsequently, they reported new values for the alignment which at their maximum were closer to the limit of $A_0^{(2)}=-1.0$.[4]

Theoretical calculations indicate that the alignment of the scattered molecules should be very high, particularly at higher J values,[4,5–7] and have shown that the alignment should be sensitive to the surface corrugation.[5] Lauderdale *et al.*[6] have pointed out that higher-order moments are necessary to provide an adequate description of the alignment for very highly aligned samples.

The angular and velocity distributions for N_2 scattered from various index planes of silver have been reported by Muhlhausen *et al.*[7] and by Asada.[8] Both groups observed broad peaks in the angular distribution near the specular angle, and interpreted this as evidence of a direct scattering process. Muhlhausen *et al.*[7] concluded that the measured angular and velocity distributions provided little information regarding rotational inelasticity or the orientational dependence of the interaction potential, and pointed out the need for direct measurements.

II. EXPERIMENT

With the exception of a few modifications, the vacuum chamber used in these experiments has been described in detail previously.[9] This chamber is equipped with low-energy electron diffraction (LEED), Auger, a sputter gun, and a quadrupole mass spectrometer for residual gas analysis. The molecular beam source is a pulsed nozzle beam (General Valve), with an orifice of 150-μm diameter, operated at stagnation pressures of 80–100 psi (gauge). Gas load on the main chamber is reduced by a mechanical chopper operated at 200 Hz with a duty factor of 1/200. Beam energies are controlled by seeding N_2 in either He or H_2. The molecular beam strikes the crystal at a variable angle of incidence. The exposed area at normal incidence is 4 mm in diameter. With the beam, on the background pressure in the main chamber is 2×10^{-10} Torr. The Ag(111) crystal (Aremco Inc.) was prepared as described previously[9] and mounted on a manipulator equipped with liquid-nitrogen cooling and electron bombardment heating.

Tunable radiation (283–285 nm) used to excite the (1,0) band of the N_2 $a\,^1\Pi_g \leftarrow X\,^1\Sigma_g^+$ two-photon transition is gen-

 0734-2101/87/040513-05$01.00

erated by frequency doubling the output of a YAG pumped dye laser (Quantel 581C-TDL50-UVX2). This produces 15–20 mJ in an 8-ns pulse with a bandwidth of ~ 0.2 cm^{-1}. The UV light is separated from the visible fundamental by a 60° dispersing prism, and directed through a second 60° prism in a mirror image configuration to the first in order to compensate for angular beam walk during a wavelength scan. A 20-cm quartz lens focuses the UV light into the vacuum chamber. The focal point is 1 cm from the surface and is located at the specular angle. The laser beam is linearly polarized and the plane of polarization is varied by means of a double Fresnel rhomb.

Due to the spot size of the molecular beam on the surface and the distance of the laser focal point from the surface, the angular resolution is $\sim 20°$. Because the direct inelastically scattered molecules are concentrated in a lobe about the specular angle, this angular resolution effectively averages over the final scattering angles.

Ions formed at the laser focus are extracted into a time-of-flight mass spectrometer and detected with a microchannel plate. A gated integrator allows for selective detection of a particular mass of interest.[10] At the same time an ion signal is measured, a signal proportional to the laser power is recorded with a pyroelectric device (Molectron P1-12). The ion signal is corrected by dividing by the square of the laser power to account for variations in laser energy during a scan.[2] The laser wavelength and polarization are scanned and the signal is accumulated under computer control. Typical acquisition times are between 15 min and 2 h.

III. RESULTS

Figure 1 shows a REMPI spectrum of the incident N_2 beam. The line assignments are made based on tabulated energy levels.[11] The distribution corresponds to a rotational "temperature" of about 5 K. Due to the presence of ortho- and paranuclear spin states in N_2 even and odd rotational levels are not collisionally mixed in either the supersonic expansion or by subsequent scattering from the surface.

Figure 2(a) displays a REMPI spectrum of N_2 scattered from Ag(111) at 200-meV incident energy, 15° incident angle, and at a surface temperature of 392 K. Shown for comparison in Fig. 2(b) is a REMPI spectrum of an isotropic background sample of N_2 (admitted to the chamber through a leak valve) at a pressure of 5×10^{-7} Torr. The difference in intensities between pairs of lines originating from a common J between spectra (a) and (b), for example, O(11) and P(11) or O(5) and P(5), is an indication that the surface-scattered molecules are not isotropic. For an anisotropic distribution of angular momenta, the different rotational branches will in general have different transition probabilities at a fixed laser polarization.

The degree of alignment of a given rotational level is determined by tuning the wavelength to a transition originating from that level and then varying the laser polarization. An example of such a measurement is shown in Fig. 3 for $J = 14$ of the O branch.

A detailed description of how molecular population and alignment parameters are determined from spectra, such as Fig. 3, is presented elsewhere[12] and will be only summarized

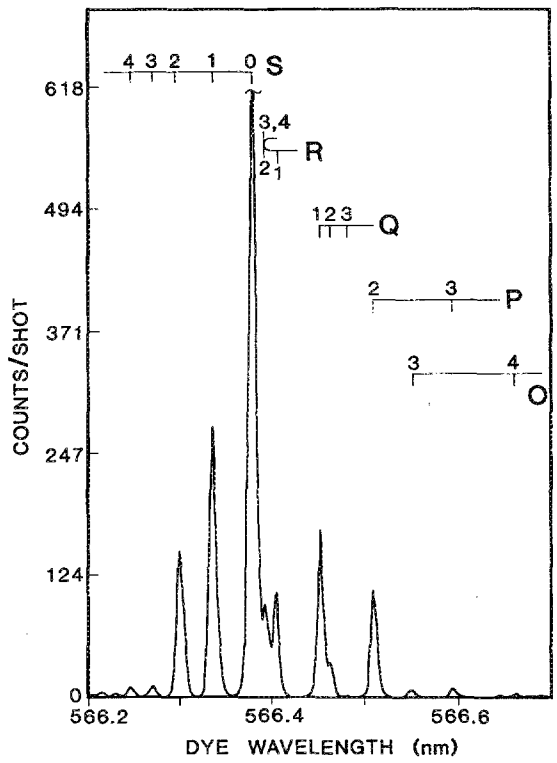

FIG. 1. 2 + 2 REMPI spectrum of the incident, supersonically cooled, N_2 beam. The population distribution corresponds to a rotational temperature of approximately 5 K.

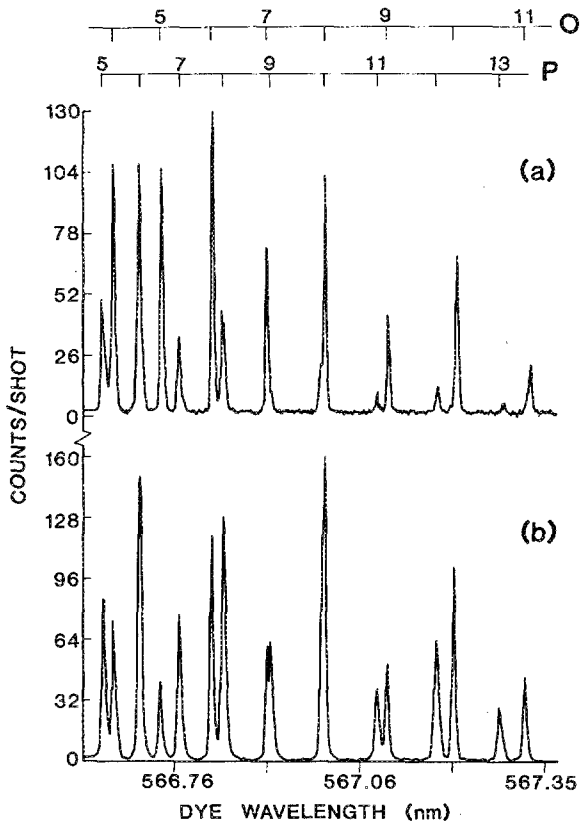

FIG. 2. A comparison of 2 + 2 REMPI spectra for (a) surface scattered N_2 and (b) an isotropic background gas of N_2 at room temperature.

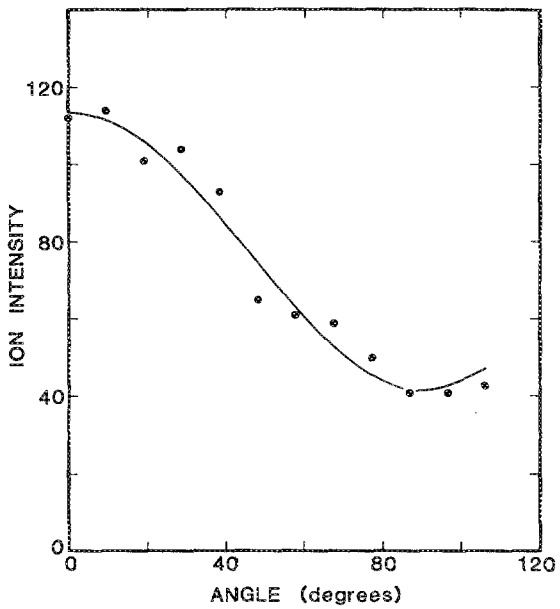

FIG. 3. Variation of ion signal vs laser polarization for $J = 14$ of the O branch. The angle is measured with respect to the surface normal. The solid curve is a least-squares fit of the data points to Eq. (1).

here briefly. Assuming the sample has cylindrical symmetry about the surface normal, the intensity of a given two-photon absorption line ($J \rightarrow J'$), at a laser polarization angle θ with respect to the surface normal $\hat{n}$, can be written

$$I(J,\theta) = CA_0^{(0)}(J)\left[P_0^0(J,J';\theta) + A_0^{(2)}(J)P_0^2(J,J';\theta) + A_0^{(4)}(J)P_0^4(J,J';\theta)\right], \quad (1)$$

where $P_0^n(J,J';\theta)$ is the rotational branch dependent line strength factor for a given excitation/detection geometry.

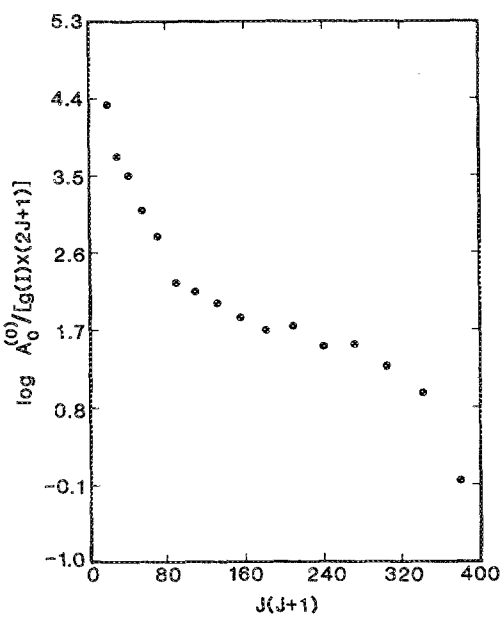

FIG. 4. A plot of the relative rotational populations divided by the nuclear spin and rotational degeneracies vs $J(J+1)$ for N_2 scattered from Ag(111). The broad feature at high J is interpreted as a rotational rainbow.

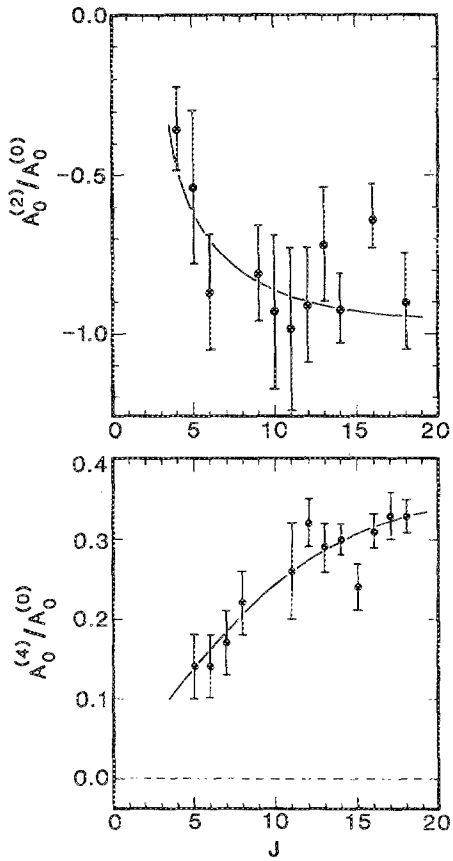

FIG. 5. Alignment moments vs J for N_2/Ag(111): (a) the quadrupole moment $A_0^{(2)}(J)$, and (b) the hexadecapole moment $A_0^{(4)}(J)$. The limiting values for J aligned perfectly parallel to the surface are $A_0^{(2)} = -1.0$, and $A_0^{(4)} = +0.375$. For no alignment $A_0^{(2)} = A_0^{(4)}(J) = 0$.

The calculation of P_0^n is detailed in Ref. 12. The $A_0^{(n)}(J)$ is the nth moment of the J angular momentum distribution. The zeroth moment $A_0^{(0)}$ is just the population of the rotational level J, while the second $A_0^{(2)}$ and fourth $A_0^{(4)}$ moments describe the spatial distribution of the vector $\mathbf{J}$, i.e., the M_J distribution where the quantization axis is the surface normal:

$$A_0^{(2)}(J) = (3J_z^2 - \mathbf{J}^2)/\mathbf{J}^2, \quad (2a)$$

$$A_0^{(4)}(J) = (3\mathbf{J}^4 - 6\mathbf{J}^2 - 30J_z^2\mathbf{J}^2 + 25J_z^2 + 35J_z^4)/8\mathbf{J}^4. \quad (2b)$$

Note that $A_0^{(2)}(J) = 2P_2(\cos\theta)$, where $\cos\theta = M_J/J(J+1)$ and for high J, $A_0^{(4)}$ approaches $P_4(\cos\theta)$.

Data, such as that shown in Fig. 3, are accumulated for each well-resolved transition. The variation of ion signal $I(J,\theta)$ with polarization angle θ is fit to expression (1) to determine $A_0^{(2)}(J)$ and $A_0^{(4)}(J)$. A wavelength scan across all the levels in conjunction with the alignment parameters for each line then serves to determine the relative populations, $A_0^{(0)}(J)$, of the rotational levels.

Results are presented in Figs. 4 and 5 for the conditions of Figs. 1 and 2(a). The results for $A_0^{(0)}(J)$ are plotted logarithmically versus $J(J+1)$, that is, in the form of a Boltzmann plot. The results for $A_0^{(2)}(J)$ and $A_0^{(4)}(J)$ are plotted on a linear scale and are normalized to $A_0^{(0)}(J)$. The limiting

values for $A_0^{(2)}$ and $A_0^{(4)}$ are $+2$ and $+1$ for $\mathbf{J}\|$ to $\hat{n}$ and -1 and $+0.375$ for $\mathbf{J}\perp$ to $\hat{n}$, while for isotropic J, $A_0^{(2)} = A_0^{(4)} = 0$. Clearly Figs. 5(a) and 5(b) show that the J distribution closely approaches the case where J is confined to a plane parallel to the scattering surface.

IV. DISCUSSION

A Boltzmann population distribution of rotational states would yield a straight line for a plot of $A_0^{(0)}(J)$ such as that given in Fig. 4. The plot of $A_0^{(0)}(J)$ for N_2 scattered from Ag(111) is clearly not linear, instead showing excess population in higher J levels and a sharp cutoff at still higher J. This behavior has been seen previously in the NO/Ag(111) system[9,13] and has been interpreted as a rotational rainbow. It arises from an extremum in the rotational excitation function versus the angle the diatom internuclear axis makes with the surface normal.

The observation of rotational rainbows for the N_2/Ag(111) system is interesting for two reasons: First, we observe rotational rainbows at considerably lower energy than in the NO/Ag(111) case. This may be due to the attractive well depth for N_2 on silver, which although not known, is presumably substantially less than that for NO. Theoretical modeling indicates that the attractive well serves to smear out a rotational rainbow.[14] Rainbow features are also blurred by the initial rotational excitation of the incident beam,[15] which for N_2 is less than for NO. In addition, most NO/Ag(111) experiments were performed at surface temperatures at or above 400 K. We have been able to work at temperatures as low as 90 K and still observe direct inelastic scattering. Higher surface temperatures are also predicted to smear out rotational rainbows.[14] Evidence that the scattering is still direct at low surface temperatures comes from measurements at different incident energies, in which we find that the observed scattered distributions are strongly dependent on the initial N_2 energy.

Second, in calculations for the NO/Ag(111) case, it was found that a strong orientationally dependent attractive interaction was necessary to produce significant rainbow features.[16] This cannot be the case for N_2 on Ag(111). Therefore the rotational rainbow feature must be due to a hard collision with the repulsive wall of the potential, a result that is predicted by several simple models.[14,15,17]

Figure 5 shows the $A_0^{(2)}(J)$ and $A_0^{(4)}(J)$ moment distributions versus J. Inspection of these results indicates that even at low J ($4 < J < 7$) the scattered sample is aligned and at higher J ($J > 7$) the alignment parameters approach their limiting values for the J vector lying parallel to the surface. The determination of $A_0^{(4)}(J)$ in the current experiment provides important information about the degree of alignment. Our plot of $A_0^{(2)}/A_0^{(0)}$ looks qualitatively very similar to results calculated by Wolf, Collins, and Mayne[5] for N_2 scattered from a rigid surface with small corrugation. There are no published results with which to compare the $A_0^{(4)}/A_0^{(0)}$ data, since to our knowledge, this is the first time the hexadecapole moment has been measured.

The moments reported here do not, of course, completely define the angular momentum distribution, so it is appropriate to ask just what information they do contain. For the purpose of illustration we will calculate the $A_0^{(2)}(J)$ and $A_0^{(4)}(J)$ moments for a model angular momentum distribution where the probability of J having a projection M_J on an axis z is given by $P(M_J) = \exp[-\alpha M_J/J]$. The parameter α controls the rate of falloff with angle, where the angle is the $\arccos(M_J/J)$. Figure 6 shows a polar plot of the distribution for two values of α and gives the values of $A_0^{(2)}(J)$ and $A_0^{(4)}(J)$ calculated in the high J limit according to Eq. (2). In the plot, the distance from the origin to the curve at a given angle is proportional to the relative probability of J lying at that angle to z. These plots are cylindrically symmetric under rotation about the z axis. Experimentally, the surface normal corresponds to the z axis. It is seen from the plot that for $\alpha = 7.50$ the J vector is constrained to lie within a very narrow angular spread perpendicular to the z axis, even for $A_0^{(2)}$ and $A_0^{(4)}$ values less than those derived from our data.

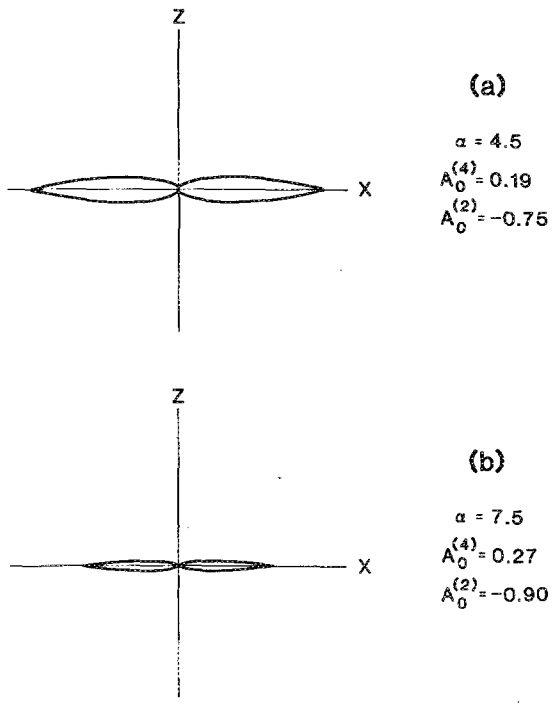

FIG. 6. Polar plots of the angular momentum distribution for a model where the probability of J having a projection M_J on the z axis is given by $P(M_J) = \exp[-\alpha M_J/J]$. Included are the $A_0^{(2)}$ and $A_0^{(4)}$ values calculated according to Eq. (2), in the high J limit.

It is concluded that the N_2/Ag(111) system closely approaches the ideal of a rigid rotor colliding with flat surface. It is hoped that the determination of the first three even moments of the angular momentum distribution for N_2 scattered from Ag(111) will provide a more stringent test of potentials currently employed in modeling gas–surface interactions. Current efforts are aimed at investigating in detail the effects of surface temperature and incident energy.

ACKNOWLEDGMENTS

This work was supported by the Army Research Office under Grant No. DAAG-29-84-K-0027, and by the Office of

Naval Research under Grant No. N00014-78-C-0403. We also are grateful for the use of the Stanford Cell Biology Computer Center under NSF Grant No. DMB 84-00396.

[1]J. A. Barker and D. J. Auerbach, Surf. Sci. Rep. **4**, 1 (1984).
[2]K. L. Carleton, K. H. Welge, and S. R. Leone, Chem. Phys. Lett. **115**, 492 (1985).
[3]A. C. Luntz, A. W. Kleyn, and D. J. Auerbach, Phys. Rev. B **25**, 4273 (1982).
[4]A. W. Kleyn, A. C. Luntz, and D. J. Auerbach, Surf. Sci. **152**, 99 (1985).
[5]R. J. Wolf, D. C. Collins, Jr., and H. R. Mayne, Chem. Phys. Lett. **119**, 533 (1985).
[6]J. G. Lauderdale, J. F. McNutt, and C. W. McCurdy, Chem. Phys. Lett. **107**, 43 (1984).
[7]C. W. Muhlhausen, J. A. Serri, J. C. Tully, G. E. Becker, and M. J. Cardillo, Isr. J. Chem. **22**, 315 (1982).
[8]H. Asada, Jpn. J. Appl. Phys. **20**, 527 (1981).
[9]G. D. Kubiak, J. E. Hurst, H. G. Rennagel, G. M. McClelland, and R. N. Zare, J. Chem. Phys. **79**, 5163 (1983).
[10]G. D. Kubiak, G. O. Sitz, and R. N. Zare, J. Chem. Phys. **83**, 2538 (1985).
[11]J. T. Vanderslice, S. G. Tilford, and P. G. Wilkinson, Astrophys. J. **141**, 395 (1965).
[12]A. C. Kummel, G. O. Sitz, and R. N. Zare, J. Chem. Phys. **85**, 6874 (1986).
[13]A. W. Kleyn, A. C. Luntz, and D. J. Auerbach, Phys. Rev. Lett. **47**, 1169 (1981).
[14]J. E. Hurst, G. D. Kubiak, and R. N. Zare, Chem. Phys. Lett. **93**, 235 (1982).
[15]J. A. Barker, A. W. Kleyn, and D. J. Auerbach, Chem. Phys. Lett. **97**, 9 (1983).
[16]C. W. Muhlhausen, L. R. Williams, and J. C. Tully, Chem. Phys. Lett. **83**, 2594 (1985).
[17]R. Schinke, J. Chem. Phys. **76**, 2352 (1982).